

Near-infrared waveguide photodetector with Ge/Si self-assembled quantum dots

M. Elkurdi, P. Boucaud,^{a)} and S. Sauvage

Institut d'Électronique Fondamentale, UMR CNRS 8622, Bâtiment 220, Université Paris-Sud, 91405 Orsay, France

O. Kermarrec, Y. Campidelli, and D. Bensahel

STMicroelectronics, 850 Rue Jean Monnet, 38926 Crolles Cedex, France

G. Saint-Girons and I. Sagnes

Laboratoire de Photonique et Nanostructures, 196 Avenue Henri Ravéra, 92222 Bagneux, France

(Received 11 July 2001; accepted for publication 9 November 2001)

We have investigated near-infrared *p-i-n* photodetectors with Ge/Si self-assembled quantum dots. The self-assembled quantum dots were grown by chemical vapor deposition on Si(001). A vertical stacking of 20 layers of quantum dots was inserted into a near-infrared waveguide obtained with a Si_{0.98}Ge_{0.02} alloy. The samples were processed into ridge waveguides. The photoresponse of the device covers the near-infrared spectral range up to 1.5 μm . At room temperature, a responsivity of 210 mA/W is measured at 1.3 μm and 3 mA/W at 1.5 μm . The photocurrent is compared to the photoluminescence and to the absorption of the quantum dots measured in the waveguide geometry. At room temperature, the onset of the absorption is around 1.9 μm (0.65 eV). The photocurrent is blueshifted as compared to the absorption. © 2002 American Institute of Physics.

[DOI: 10.1063/1.1435063]

Silicon germanium alloys exhibit a lower band gap than silicon.¹ Many attempts were undertaken in recent years to use SiGe alloys for near-infrared optoelectronic applications.² One of the major goals was to develop near-infrared photonic devices operating at the telecommunication wavelengths of 1.3 and 1.55 μm . The integration of SiGe on a silicon chip and its compatibility with silicon-based electronic circuitry presents a high potential in terms of low-cost optoelectronic modules. Several types of near infrared photodetectors were developed recently with thick or two-dimensional SiGe alloy layers epitaxially deposited on silicon.³ Avalanche gain in *n⁺-p-p⁺*Ge_xSi_{1-x}/Si waveguide photodetectors was reported.⁴ The lattice mismatch between Si and SiGe limits however the deposited thickness to a critical value before the onset of the dislocation nucleation. The telecommunication wavelengths of 1.3 and 1.55 μm are therefore difficult to reach with the standard growth since high-germanium content layers are required for these applications. The operation of detectors at 1.3 μm can be obtained with strained-layer superlattices like Ge_{0.6}Si_{0.4} (Ref. 5) or Ge_{0.5}Si_{0.5} (Ref. 6). Recently, the growth of undulating Si_{0.5}Ge_{0.5} layers was proposed to reach the 1.55 μm wavelength.⁷ Metal–semiconductor–metal photodetectors were realized with a vertical stacking of undulated layers. A photoresponse of 0.1 A/W at 1.55 μm was measured at room temperature with this system. The deposition of pure Ge layers represents another alternative. A first realization of a pure Ge *p-i-n* photodetector grown on a graded alloy layer deposited on silicon was reported in 1986.⁸ However, a high dislocation density was present, inducing a strong dark current. More recently, the deposition of pure Ge layers by

chemical vapor deposition at low temperature followed by postgrowth cyclic thermal annealing was reported.⁹ The thermal treatment which reduces the threading-dislocation density considerably improves the performances leading to a responsivity of 550 mA/W at 1.32 μm and 250 mA/W at 1.55 μm .

Another route to grow high-germanium content layers relies on the Stranski–Krastanow growth of pure Ge on Si.¹⁰ This growth regime leads to the formation of coherent nanometer-size islands or quantum dots for a deposited thickness of Ge greater than a critical thickness (\sim 4 monolayers). These self-assembled quantum dots exhibit a photoluminescence around 1.3 – 1.5 μm and are therefore appropriate candidates for near-infrared devices like emitters or detectors. The quantum dots are covered by pseudomorphic silicon, allowing in turn vertical integration with Si, which is not the case for Ge-terminated surfaces. Photodetectors using a vertical stacking of seven self-assembled quantum dot layers were first reported in Ref. 11. In a normal incidence geometry, the interaction length between the light and the quantum dot layers remains quite small, thus leading to a low absorption efficiency and to a low responsivity. An increased interaction length can be obtained with a waveguide geometry. Several types of near-infrared waveguides can be fabricated on silicon, in particular with silicon-on-insulator substrates. Waveguides with a weak confinement can also be obtained with thick SiGe alloys with a small germanium content. SiGe alloys with a small Ge content offer the advantage to be transparent at the 1.3 and 1.55 μm telecommunication wavelengths.¹²

In this work, we report on near-infrared waveguide detectors using Ge/Si self-assembled quantum dots in the optical active region. The detector consists of *p-i-n* diodes with

^{a)}Electronic mail: phil@ief.u-psud.fr

quantum dots embedded in a $\text{Si}_{0.98}\text{Ge}_{0.02}$ layer. At room temperature, a responsivity of 210 and 3 mA/W are measured at $1.3\ \mu\text{m}$ and $1.5\ \mu\text{m}$, respectively. The interband absorption of the Ge/Si self-assembled dot layers is measured.

The self-assembled quantum dots were grown in an industrial lamp-heated single wafer chemical vapor deposition reactor.^{13,14} The wafers were 200 mm diameter (001) oriented Si substrates. Silane and germane diluted in hydrogen carrier gas were used as gas precursors. The process temperature deposition was around $700\ ^\circ\text{C}$, at a total pressure lower than 100 Torr. The photodetector structure was the following: a $2\ \mu\text{m}$ thick $\text{Si}_{0.98}\text{Ge}_{0.02}$ layer, a $200\ \text{nm}$ thick p^+ Si layer *in situ* doped with Boron ($10^{19}\ \text{cm}^{-3}$) using B_2H_6 diluted in H_2 , a $80\ \text{nm}$ thick $\text{Si}_{0.98}\text{Ge}_{0.02}$ spacer layer, 20 self-assembled quantum dot layers separated by $50\ \text{nm}$ thick $\text{Si}_{0.98}\text{Ge}_{0.02}$ barrier layers, a $80\ \text{nm}$ thick $\text{Si}_{0.98}\text{Ge}_{0.02}$ spacer layer, and a $100\ \text{nm}$ thick n^+ contact layer *in situ* doped with phosphine diluted in H_2 ($10^{19}\ \text{cm}^{-3}$). The growth of a 2% SiGe layer provides a weak confinement of the light due to the variation of the optical refractive index ($\Delta n \sim 6 \times 10^{-3}$). The dot density is around $2.6 \times 10^9\ \text{cm}^{-2}$, i.e., lower than the density reported in Ref. 13. The dome-shaped quantum dots observed in a single Ge layer grown in the same conditions (i.e., uncapped quantum dots) have a typical base size of $160\ \text{nm}$ and a height of $23\ \text{nm}$. After capping by silicon, the confinement of the carriers in the islands leads to a confinement energy of a few meV in the layer plane and a few tens of meV along the growth direction.¹⁵ A sample without quantum dots was grown as a reference for absorption measurements. Devices without waveguides operating at normal incidence were used in order to measure the photoresponse of a silicon $p-i-n$ diode.¹⁶

The detectors were processed by reactive ion etching into $100\ \mu\text{m}$ thick ridge waveguides. The etch depth was $1.4\ \mu\text{m}$. Devices with lengths going from 3 to 7 mm were measured. The ohmic contacts with the p^+ and the n^+ layers were obtained by depositing Ti/Au contacts. The detectors were glued to a ceramic pedestal. The top and back contacts were bonded with gold wires using standard thermocompression bonding. The photoluminescence spectra were measured with a liquid-nitrogen cooled Ge photodiode. The photoluminescence was excited with an Ar^+ laser. The spectral response of the devices was measured with a microscope coupled to a Fourier-transform infrared spectrometer.

Figure 1 shows the low temperature photoluminescence spectrum of the quantum dot sample. The dominant recombination line resonant at $1.53\ \mu\text{m}$ is attributed to the Ge/Si self-assembled quantum dots. The broadening of $0.18\ \mu\text{m}$ at half width at half maximum is attributed to the dispersion of composition and size within a layer and to an additional dispersion introduced by the vertical stacking. We note that the relatively high excitation power of $400\ \text{mW}$ induces an additional broadening due to the dot filling.¹⁵ The broad radiative recombination is typical of Ge/Si self-assembled quantum dots^{17–19} and significantly different from the dislocation-related photoluminescence spectra in silicon.²⁰ A weak recombination is observed at 1.24 and $1.32\ \mu\text{m}$. We associate these lines with the recombination in the wetting layers even if these recombination lines are resonant at energies close to that of the D3 and D4 dislocations in silicon.

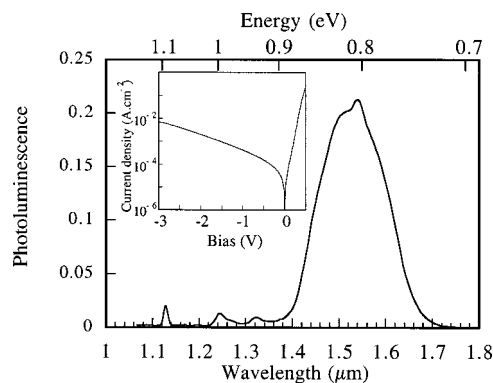


FIG. 1. Low-temperature (5 K) photoluminescence spectrum of the waveguide with Ge/Si self-assembled quantum dots. The inset shows the room-temperature current density–voltage characteristic of a 7 mm long device.

Separate measurements on different samples show that these lines shift in energy for different growth conditions. The phonon-assisted recombination in the silicon substrate is evidenced at $1.127\ \mu\text{m}$. We did not observe a signature of the $\text{Si}_{0.98}\text{Ge}_{0.02}$ core of the waveguide, thus indicating an efficient transfer of the optically excited carriers to the quantum dots. The inset of Fig. 1 shows the room-temperature current density–voltage characteristic of a 7 mm long device. For a reverse applied bias of $-1\ \text{V}$, a dark current of $2.8\ \mu\text{A}$ ($4.2 \times 10^{-4}\ \text{A cm}^{-2}$) is measured at room temperature.

The photoresponse of a 7 mm long device measured at room temperature is shown in Fig. 2. The applied bias is $0\ \text{V}$ and the photocurrent is measured in a short circuit configuration. The photoresponse of a Si $p-i-n$ diode grown in the same growth chamber is given as reference. In the latter case, a normal incidence geometry was used. The cutoff wavelength of the silicon photodiode is around $1.2\ \mu\text{m}$. The spectral response of the waveguide detector with self-assembled quantum dots clearly covers a broader spectral range. As expected, the spectral response can be measured up to $1.5\ \mu\text{m}$ wavelength due to the high germanium content of the self-assembled layers. The spectral response was calibrated without accounting for the weak coupling efficiency into the waveguide (i.e., conservative values are given). Responsivities of 210 mA/W and 3 mA/W were measured at $1.3\ \mu\text{m}$ and $1.5\ \mu\text{m}$, respectively. We did not observe any significant dependence of the photocurrent on the polarization of the incoming light. This feature is in strong contrast to the results reported for InAs/GaAs self-assembled quantum dots

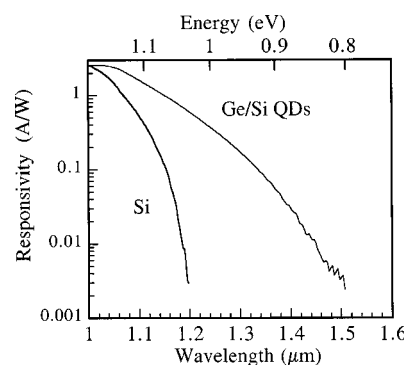


FIG. 2. Room-temperature responsivity of the waveguide photodetector. The applied bias is $0\ \text{V}$. The response of a silicon $p-i-n$ photodiode is given as a reference.

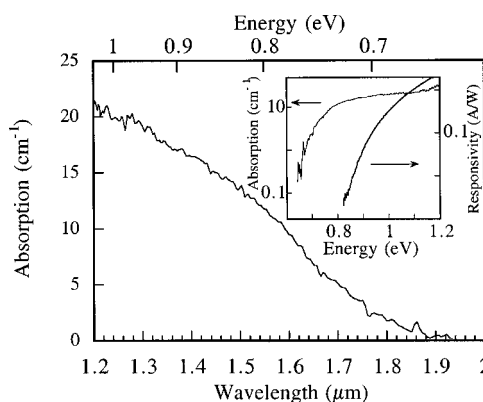


FIG. 3. Room-temperature absorption measured with a $900\text{ }\mu\text{m}$ long waveguide structure. The inset shows a comparison at room temperature between the absorption and the photocurrent (energy scale).

where the photocurrent at low energy was only observed for transverse electric (TE) polarized light.²¹ We note that the amplitude of the photocurrent is weakly dependent on the applied bias. Similar results were obtained for 3 or 7 mm long devices since these lengths are larger than the absorption length of the waveguide.

Figure 3 shows the absorption of a $900\text{ }\mu\text{m}$ long waveguide quantum dot sample. The absorption is obtained by normalizing the transmission of the quantum dot sample by the transmission of a waveguide reference sample with a shorter length. The measurement was performed at room temperature. We have carefully checked with samples with different lengths the origin of the absorption. The onset of the absorption occurs around $1.9\text{ }\mu\text{m}$ (0.65 eV). The quantitative measurement of the absorption coefficient of the quantum dot layers is difficult because of the weak confinement of the waveguide and the uncertainty on the overlap factor between the guided optical modes and the quantum dot layers. A detailed discussion of the absorption and the comparison of its energy dependence with the usual laws for the absorption of an indirect gap bulk semiconductor using the Macfarlane–Roberts expression¹ or the absorption of a two-dimensional indirect gap semiconductor²² are beyond the scope of this work. Only a rough estimation of the absorption coefficient can be given: if we assume an overlap factor of 1.3×10^{-2} between the quantum dot layers and the first confined optical mode²³ an absorption coefficient of 1000 cm^{-1} is measured at $1.5\text{ }\mu\text{m}$ for one quantum dot layer. The onset of the absorption can be compared to that reported for strained $\text{Si}_{1-x}\text{Ge}_x$ layer structures at low temperature (90 K).²⁴ A variation of the onset of the absorption of approximately 70 meV can be assumed between room temperature and 90 K. At 90 K, the onset of the absorption is therefore predicted to occur around 720 meV. This value, which accounts for the weak confinement energy of the dots, is close to that reported for a strained $\text{Si}_{0.4}\text{Ge}_{0.6}$ alloy in Ref. 24. A similar alloy concentration is deduced following the theoretical approach by in Ref. 25 by People to estimate the band gap of coherently strained $\text{Ge}_x\text{Si}_{1-x}$ bulk alloys. This feature indicates that the absorption properties of the self-assembled quantum dots are similar to that of a tetragonally strained $\text{Si}_{0.4}\text{Ge}_{0.6}$ alloy layer. We emphasize that selected-area elec-

tron diffraction measurements on single buried quantum dots grown by chemical vapor deposition did predict an average composition of 50% for the quantum dots, as a result of strain-induced intermixing.²⁶ These two values obtained by the analysis of the structural and of the optical properties are thus found consistent.

We can notice that the onset of the absorption of the quantum dots is close to that of a bulk Ge layer. This similarity is associated with the strain field which lowers significantly the band gap. The photocurrent is blueshifted as compared to the absorption. As the photocurrent results from a convolution of the absorption and of the tunneling probabilities of the carriers, this blueshift is not surprising. The tunneling probabilities of the carriers is higher for carriers close to the band edge. Finally, we note that the onset of the absorption corresponds to the onset of the photoluminescence of the quantum dot layers.

This work was supported by the Réseau Micro et Nanotechnologie (RMNT) under Contract No. 00V0091.

- ¹R. Braunstein, A. R. Moore, and F. Herman, Phys. Rev. **109**, 695 (1958).
- ²R. People, IEEE J. Quantum Electron. **22**, 1696 (1986).
- ³H. Temkin, J. C. Bean, T. P. Pearsall, N. A. Olsson, and D. V. Lang, Appl. Phys. Lett. **49**, 155 (1986).
- ⁴T. P. Pearsall, H. Temkin, J. C. Bean, and S. Luryi, IEEE Electron Device Lett. **7**, 330 (1986).
- ⁵H. Temkin, A. Antreasyan, N. A. Olsson, T. P. Pearsall, and J. C. Bean, Appl. Phys. Lett. **49**, 809 (1986).
- ⁶F. Y. Huang, X. Zhu, M. O. Tanner, and K. L. Wang, Appl. Phys. Lett. **67**, 566 (1995).
- ⁷H. Lafontaine, N. L. Rowell, S. Janz, and D. X. Xu, J. Appl. Phys. **86**, 1287 (1999).
- ⁸S. Luryi, A. Kastalsky, and J. C. Bean, IEEE Trans. Electron Devices **31**, 1135 (1984).
- ⁹L. Colace, G. Masini, G. Assanto, H. C. Luan, K. Wada, and L. C. Kimerling, Appl. Phys. Lett. **76**, 1231 (2000).
- ¹⁰D. E. Eaglesham and M. Cerullo, Phys. Rev. Lett. **64**, 1943 (1990).
- ¹¹G. Abstreiter, P. Schittenhelm, C. Engel, E. Silveira, A. Zrenner, D. Meertens, and W. Jäger, Semicond. Sci. Technol. **11**, 1521 (1996).
- ¹²B. Schüppert, J. Schmidtchen, A. Splett, U. Fischer, T. Zinke, R. Moosburger, and K. Petermann, J. Lightwave Technol. **14**, 2311 (1996).
- ¹³C. Hernandez, Y. Campidelli, D. Simon, D. Bensahel, I. Sagnes, G. Patriarche, P. Boucaud, and S. Sauvage, J. Appl. Phys. **86**, 1145 (1999).
- ¹⁴D. Bensahel, Y. Campidelli, C. Hernandez, F. Martin, I. Sagnes, and D. J. Meyer, Solid State Technol. **41**, S5 (1998).
- ¹⁵P. Boucaud, S. Sauvage, M. Elkurdi, E. Mercier, T. Brunhes, V. Le Thanh, and D. Bouchier, Phys. Rev. B **64**, 155310 (2001).
- ¹⁶T. Brunhes, P. Boucaud, S. Sauvage, F. Aniel, J.-M. Lourtioz, C. Hernandez, Y. Campidelli, D. Bensahel, G. Faini, and I. Sagnes, Appl. Phys. Lett. **77**, 1822 (2000).
- ¹⁷P. Schittenhelm, M. Gail, J. Brunner, J. F. Nützel, and G. Abstreiter, Appl. Phys. Lett. **67**, 1292 (1995).
- ¹⁸O. G. Schmidt, C. Lange, and K. Eberl, Appl. Phys. Lett. **75**, 1905 (1999).
- ¹⁹V. Le Thanh, V. Yam, P. Boucaud, F. Fortuna, C. Ulysse, D. Bouchier, L. Vervoort, and J.-M. Lourtioz, Phys. Rev. B **60**, 5851 (1999).
- ²⁰R. Sauer, J. Weber, J. Stolz, E. R. Weber, K.-H. Küsters, and H. Alexander, Appl. Phys. A: Mater. Sci. Process. **36**, 1 (1985).
- ²¹L. Chu, M. Arzberger, A. Zrenner, G. Böhm, and G. Abstreiter, Appl. Phys. Lett. **75**, 2247 (1999).
- ²²P. K. Basu and S. K. Paul, Phys. Rev. B **46**, 13389 (1992).
- ²³S. Sauvage, P. Boucaud, F. Glotin, R. Prazeres, J. M. Ortega, A. Lemaitre, J. M. Gérard, and V. Thierry-Mieg, Appl. Phys. Lett. **73**, 3818 (1998).
- ²⁴D. V. Lang, R. People, J. C. Bean, and A. M. Sergent, Appl. Phys. Lett. **47**, 1333 (1985).
- ²⁵R. People, Phys. Rev. B **32**, 1405 (1985).
- ²⁶G. Patriarche, I. Sagnes, P. Boucaud, V. Le Thanh, D. Bouchier, C. Hernandez, Y. Campidelli, O. Kermarrec, and D. Bensahel, Appl. Phys. Lett. **77**, 370 (2000).